methods

Functional recombinant apolipoprotein A5 that is stable at high concentrations at physiological pH[S]

Mark Castleberry,* Xenia Davis,† Min Liu,† Thomas B. Thompson,* Patrick Tso,† and W. Sean Davidson[1,†]

Departments of Molecular Genetics, Biochemistry, and Microbiology* and Pathology and Laboratory Medicine,† University of Cincinnati College of Medicine, Cincinnati, OH

ORCID ID: 0000-0002-7041-5047 (T.B.T.); 0000-0003-2756-2989 (W.S.D.)

Abstract **APOA5 is a low-abundance exchangeable apolipoprotein that plays critical roles in human triglyceride (TG) metabolism. Indeed, aberrations in the plasma concentration or structure of APOA5 are linked to hypertriglyceridemia, hyperchylomicronemia, myocardial infarction risk, obesity, and coronary artery disease. While it has been successfully produced at low yield in bacteria, the resulting protein had limitations for structure-function studies due to its low solubility under physiological buffer conditions. We hypothesized that the yield and solubility of recombinant APOA5 could be increased by: *i*) engineering a fusion protein construct in a codon optimized expression vector, *ii*) optimizing an efficient refolding protocol, and *iii*) screening buffer systems at physiological pH. The result was a high-yield (25 mg/l) bacterial expression system that produces lipid-free APOA5 soluble at concentrations of up to 10 mg/ml at a pH of 7.8 in bicarbonate buffers. Physical characterization of lipid-free APOA5 indicated that it exists as an array of multimers in solution, and far UV circular dichroism analyses show differences in total α-helicity between acidic and neutral pH buffering conditions.** The protein was functional in that it bound and emulsified multilamellar dimyristoyl-phosphatidylcholine vesicles and could inhibit postprandial plasma TG accumulation when injected into C57BL/6J mice orally gavaged with Intralipid.—Castleberry, M., X. Davis, M. Liu, T. B. Thompson, P. Tso, and W. S. Davidson. **Functional recombinant apolipoprotein A5 that is stable at high concentrations at physiological pH. *J. Lipid Res.* 2020.** 61: **244–251.**

Supplementary key words lipoproteins • lipid and lipoprotein metabolism • triglycerides • dyslipidemias

APOA5 is an exchangeable apolipoprotein that has been implicated as a potent regulator of triglyceride (TG) and lipoprotein metabolism. In 2001, Pennacchio et al. (1) demonstrated that mice lacking APOA5 exhibited 4-fold higher circulating TGs compared with WT mice. In humans, APOA5 is expressed primarily in the liver and is secreted from hepatocytes into the plasma as an ∼39 kDa protein after the cleavage of its signal sequence. Once in the plasma, APOA5 is primarily associated with HDLs; however, it is also found on TG-rich lipoprotein particles (i.e., VLDLs, chylomicrons) (2). Previous studies have suggested that APOA5 regulates TG metabolism through multiple mechanisms including: acceleration of heparin-bound lipoprotein lipase-mediated hydrolysis of TG-rich lipoproteins (3); acceleration of receptor mediated uptake of TG-rich lipoproteins (4); and alteration of the secreted lipid cargo of TG-rich lipoproteins from the liver (5). APOA5 appears to have potent effects on plasma TG levels given its low circulating concentration of 104–254 ng/ml (6). In fact, APOA5 circulates at an ∼1,000-fold lower plasma concentration than APOB100 and ∼10,000-fold lower than APOA1 on a molar basis. This has led to much speculation on how APOA5 physically interacts with lipoproteins and the components of the lipid hydrolyzing machinery in plasma (7).

Despite the significant knowledge gained in previous studies, we lack detailed understanding of the mechanism(s) of action of APOA5, in part due to difficulties obtaining sufficient quantities of properly folded APOA5 protein. Although it can be isolated from plasma (8), researchers have utilized exogenous expression systems as a cheaper and more efficient alternative for acquiring significant amounts of APOA5 for structural and functional analyses (2, 9–12). Beckstead et al. (12) successfully expressed APOA5 in bacteria, and this system was used to generate much of what we

This research was supported by National Institutes of Health, National Heart, Lung, and Blood Institute Grant HL125204-03 (predoctoral fellowship to M.C.). The content is solely the responsibility of the authors and does not necessarily represent the official views of the National Institutes of Health. The authors declare that they have no conflicts of interest with the contents of this article.

Manuscript received 30 April 2019 and in revised form 25 November 2019.

Published, JLR Papers in Press, December 12, 2019
DOI https://doi.org/10.1194/jlr.D119000103

Abbreviations: BS^3, bis(sulfosuccinimidyl) suberate; CD, circular dichroism; DMPC, dimyristoyl-phosphatidylcholine; LB, Luria-Bertani; OD, optical density; SEC, size exclusion chromatography; tAPOA5, tagged APOA5; TEV, tobacco etch virus; TG, triglyceride; TRX, thioredoxin.

[1]To whom correspondence should be addressed.
e-mail: davidswm@ucmail.uc.edu

[S] The online version of this article (available at https://www.jlr.org) contains a supplement.

currently understand about APOA5 structure (13). However, the system had a significant drawback in that the product protein was essentially insoluble at physiological pH when lipid-free. As a result, most structural studies of this material were performed at acidic pH or in complex with lipid or detergent. The relatively low recombinant expression yield and solubility requirements also complicated the application of structural techniques, such as X-ray crystallography, small angle X-ray scattering, and chemical cross-linking. We hypothesized that the yield and neutral pH solubility of recombinant APOA5 could be increased by: *i*) engineering a fusion protein construct in a codon-optimized expression vector, *ii*) optimizing an efficient refolding protocol, and *iii*) screening buffer systems for optimal APOA5 solubility at physiological pH. Here, we describe a high-yield (6.4×10^{-10} mol/l; 25 mg/l) bacterial expression system that allows for the purification of lipid-free APOA5 that is soluble at high concentrations under physiological buffer conditions. A protocol suitable for routine laboratory use is provided in the supplemental materials.

MATERIALS AND METHODS

Expression of APOA5

APOA5 protein expression was performed in ClearColi® BL21(DE3) *Escherichia coli* cells (Research Corporation Technologies, Inc.). This cell line produces genetically modified LPS, which does not trigger a NF-κB-driven endotoxic response. Cells were grown in Luria-Bertani (LB) culture media, which included ampicillin (2.8 μM) as a selection agent for pET32a(+) transformants. Briefly, 100 ml LB starter cultures were inoculated with a single colony from an LB agar plate and grown to an optical density $(OD)_{600}$ of 0.8 at 37°C. Starter cultures were used to inoculate expression cultures at 1:100 v/v and grown at 37°C in baffled flasks shaking at 225 rpm. At an OD_{600} of 0.8, expression cultures were placed on ice for 15 min prior to induction with 0.4 mM isopropyl β-D-1-thiogalactopyranoside. After 16 h of expression at 25°C, cells were pelleted by centrifugation (9,800 *g*) and resuspended in 15 ml/l culture volume with a Tris-HCl buffer (20 mM Tris-HCl, 0.5 M NaCl, 0.1 mM PMSF, 1 μM leupeptin, 1 μM pepstatin A, pH 7.8).

Purification of APOA5

All purification steps were performed at 4°C. Bacterial cells were lysed by sonication and, after centrifugation (23,000 *g*), the insoluble fraction (pellet) was isolated for subsequent purification. Utilizing a denaturing Tris-HCl buffer (20 mM Tris-HCl, 0.5 M NaCl, 6 M Urea, 20 mM imidazole, pH 7.8), recombinant protein from the insoluble fraction was solubilized with agitation. After centrifugation (23,000 *g*), the soluble fraction containing denatured recombinant protein was decanted for purification via nickel affinity chromatography. The filtered cell extract was applied to a gravity column containing Ni Sepharose (GE Healthcare) high performance affinity media and purified under denaturing conditions. Utilizing a stepwise increase of imidazole during affinity purification, the protein was washed (60 mM) and eluted (1 M) from the column. Elution fractions were pooled and dialyzed into a denaturing HEPES buffer (10 mM HEPES, 150 mM NaCl, 4 M urea, pH 7.8) prior to purification via size exclusion chromatography (SEC) utilizing a HiLoad 16/600 Superdex 200 prep grade column (GE Healthcare) with a 5 ml injection volume. Elution fractions containing monomeric recombinant protein were pooled and diluted to a protein concentration of 0.2 mg/ml and then rapidly diluted 1:1 v/v to 2 M urea with a HEPES buffer (10 mM HEPES, 150 mM NaCl, pH 7.8). After a 2 h incubation, samples were dialyzed into a bicarbonate buffer (10 mM ammonium bicarbonate, 5 mM DTT, pH 7.8) prior to concentration via Bioseparations Stirred Cells (Amicon) to a concentration of 1 mg/ml. To remove N-terminal fusion tags, recombinant protein was digested with tobacco etch virus (TEV) protease at a 20:1 w/w ratio of protein to protease for 6 h and then dialyzed into a denaturing Tris-HCl buffer (20 mM Tris-HCl, 0.5 M NaCl, 6 M urea, 20 mM imidazole, pH 7.8). The digested protein sample was then applied to a nickel affinity column and flow-through fractions containing APOA5 were pooled, diluted to a concentration of 0.1 mg/ml, and dialyzed into a denaturing bicarbonate buffer (10 mM ammonium bicarbonate, 4 M urea, pH 7.8). Utilizing a stepwise dialysis procedure into our nondenaturing bicarbonate buffer (10 mM ammonium bicarbonate, 5 mM DTT, pH 7.8), the urea concentration of the protein sample was brought to 3, 2, 1, and 0 M urea in 4 h increments, using 20× the sample volume. See supplemental Methods for a detailed purification protocol and supplemental Table S1 for a purification analysis of APOA5 yield and purity at each stage of purification.

Chemical cross-linking

Recombinant APOA5 was cross-linked with bis(sulfosuccinimidyl) suberate (BS^3) (Pierce), a homobifunctional cross-linker that contains an amine-reactive N-hydroxysulfosuccinimide ester at each end of an eight carbon (11.4 Å) spacer arm. The BS^3 stock solution (6.5 mg/ml) was prepared in the bicarbonate reaction buffer (10 mM sodium bicarbonate, 5 mM DTT, pH 7.8) and added to the protein sample within 1 min to minimize hydrolysis of free cross-linker. APOA5 (0.27 mg/ml) was cross-linked at a molar ratio of 10:1 [BS^3: APOA5 (Lys)]. The reaction proceeded for 16 h at 4°C and was quenched by the addition of Tris-HCl (25 mM final concentration).

Circular dichroism spectroscopy

Circular dichroism (CD) measurements were performed on an AVIV 215 spectropolarimeter. Samples at an equal protein concentration (0.28 mg/ml) were analyzed in a 0.01 cm cuvette from 178 to 300 nm at a rate of 1 nm/s at 20°C with a bandwidth of 1 nm. Protein concentration values were confirmed by A280 measurements after dialysis into either a bicarbonate (10 mM ammonium bicarbonate, 1 mM TCEP, pH 7.8) or citrate (50 mM sodium citrate dihydrate, 45 mM citric acid, 1 mM TCEP, pH 3.0) buffer. Data were analyzed with CDSSTR (14), reference set 4, on DichroWeb (15), utilizing a mean residue weight of 113.59 Da. Results were expressed as the mean residual ellipticity for technical triplicates from two independent protein preparations.

Liposome clearance assay

Dimyristoyl-phosphatidylcholine (DMPC) multilamellar liposomes were generated immediately prior to analysis by combining N_2-dried DMPC (Avanti Polar Lipids; 850345) with a bicarbonate buffer (10 mM ammonium bicarbonate, 5 mM DTT, pH 7.8) at 5 mg/ml using brief sonication. Recombinant protein, liposomes, and buffer were quickly mixed at a DMPC to protein mass ratio of 2.5:1, with a final protein concentration of 0.17 mg/ml. The decrease in the solution turbidity was monitored over 30 min at 24.5°C by measuring a reduction in absorbance at 325 nm every 15 s. The data are expressed as a normalized OD, which was calculated by dividing the sample OD by the initial sample OD (OD_o) for five replicates of each sample.

Animal models and plasma TG analysis

Adult male C57BL/6J mice (10–12 weeks old; Jackson Laboratory, Bar Harbor, ME) were individually housed in a temperature-controlled vivarium on a 12 h light/dark cycle. Rodent chow (Teklad; Harlan) and water were provided ad libitum except where noted. All animal procedures were conducted in accordance with the National Institutes of Health Guidelines for the Care and Use of Animals and approved by the University of Cincinnati Institutional Animal Care and Use Committee. The mice were fasted for 5 h prior to receiving an intravenous injection of either lipid-free fusion-tagged APOA5 (tAPOA5) (0.7 μg/g body weight at 0.18 mg/ml) or vehicle as a control through the lateral tail vein. One hour later, all mice were orally gavaged with 10% Intralipid (15 μl/g body weight; Sigma). Blood was collected before and at 0.5, 1, 2, and 3 h after intravenous injection (n = 5 per group) via tail vein. Cellular components were removed from plasma via centrifugation at 3,000 *g* for 10 min in a tabletop centrifuge at 4°C. Plasma samples were stored at 4°C until plasma TGs were analyzed via a commercial TG assay (Randox TR210) according to manufacturer's protocol in duplicates for each time point.

RESULTS

As outlined above, previously established methods for producing recombinant human APOA5 suffered from low yield and poor protein solubility at neutral pH. We set out to solve these issues by: *i*) engineering a fusion protein construct in a codon-optimized expression vector, *ii*) optimizing an efficient refolding protocol, and *iii*) screening buffer systems at physiological pH.

Enhancement of APOA5 expression

Because different organisms exhibit unique codon usage preferences during protein translation, our first step was to optimize all codons in the human APOA5 sequence for *E. coli*-based translation. Next, we hypothesized that the addition of fusion protein tags on the N terminus of the mature APOA5 sequence would enhance expression yield, either by stabilizing mRNA transcripts or the translated protein itself. cDNA for mature APOA5 (amino acids 24-366), lacking its pro-sequence (8), was codon optimized (16) for expression in *E. coli* (supplemental Fig. S1) and cloned into the pET32a(+) vector (Novagen plasmid 69015-3) utilizing the *Nco*I and *Hin*dIII restriction enzyme sites (**Fig. 1**). This expression construct included a thioredoxin (TRX) tag, commonly used to enhance the solubility and thermal stability of recombinant proteins expressed in *E. coli* (17). In addition, the fusion construct contained a His-tag for facile purification as well as an S-tag. A TEV protease cleavage site (ENLYFQ/G) was cloned into the expression plasmid immediately upstream of the APOA5 encoding DNA. To maintain efficient TEV cleavage activity, an additional glycine residue was left on the immediate N terminus of the APOA5 sequence (Fig. 1). In previous work, the inclusion of this residue did not affect the functionality of the related proteins, APOA1 and APOA4 (18). This construct was compared with the parent pET20b(+) version with respect to APOA5 expression using the protocol listed in the Materials and Methods. Consistent with the results of Beckstead et al. (12), we found that the pET20b(+) system produced detectable levels of APOA5 (**Fig. 2**). However, the expression was enhanced about 5- to 8-fold in the pET32a(+) system. The apparent molecular mass of this product was ~57 kDa, consistent with the size of mature APOA5 and its fusion tags. Thus, we moved forward with the generation of purification and refolding protocols for this construct.

Affinity and SEC purification

Analysis of the bacterial cell lysate after sonication indicated that the majority of the tAPOA5 was sequestered into inclusion bodies, as soluble tAPOA5 was minimally detectable in the supernatant. tAPOA5 was solubilized from the lysate pellet using a urea-based denaturing buffer with subsequent centrifugation to isolate insoluble cell debris from the solubilized protein fraction (see the Materials and Methods). The solubilized cell lysate was applied to a nickel affinity column (maintained under denaturing conditions throughout), washed, and elution fractions containing the His-tagged recombinant protein were pooled. **Figure 3** shows that the ~57 kDa band was the major protein retained. SEC was used to further purify the protein (again maintained under denaturing conditions throughout). **Figure 4** shows SEC fractions of monomeric tAPOA5, which eluted between fraction volumes 54 and 69 ml.

Protein refolding and concentration

Due to the limited solubility of lipid-free APOA5 under physiological conditions, most previous work studied the protein at pH 3.0 (12). We hypothesized that APOA5 may be misfolded during bacterial expression and this may contribute to its lack of solubility at a neutral pH. Therefore, we set out to devise a denaturation/refolding protocol that would gradually allow the protein time to refold to a near native conformation. We started by refolding tAPOA5 isolated from His-Tag affinity columns (Fig. 3). Utilizing a

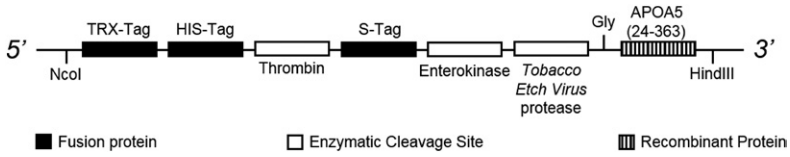

Fig. 1. Recombinant APOA5 expression vector diagram. Expression vector diagram of APOA5 in a modified pET32a(+) expression system. The codon-optimized human APOA5 (amino acids 24-366) gene was cloned into the pET32a(+) bacterial expression vector utilizing the *Nco*I and *Hin*dIII restriction enzyme sites. The TEV protease cleavage site (ENLYFQ/G) was cloned into the expression plasmid immediately upstream of the APOA5 encoding DNA.

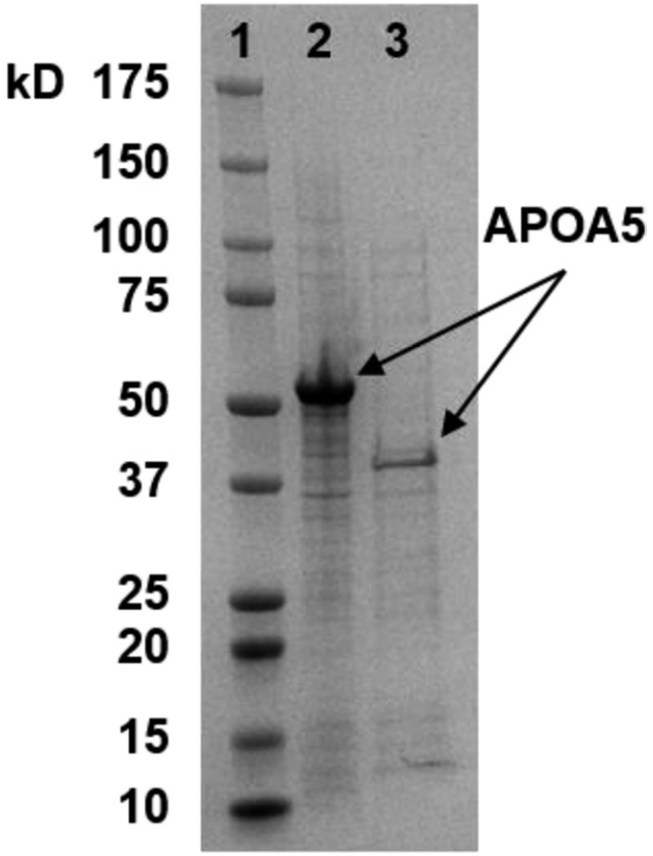

Fig. 2. Comparison of recombinant APOA5 expression. Recombinant protein expression of APOA5 mediated by pET32a(+) and pET20b(+) expression systems were analyzed by 4–15% SDS-PAGE and visualized with Coomassie blue. Cell lysates were loaded by equal volume: lane 1, low molecular mass protein standards; lane 2, pET32a(+) cell lysate (new system derived in this work); lane 3, pET20b(+) cell lysate [system used previously by Beckstead et al. (12)].

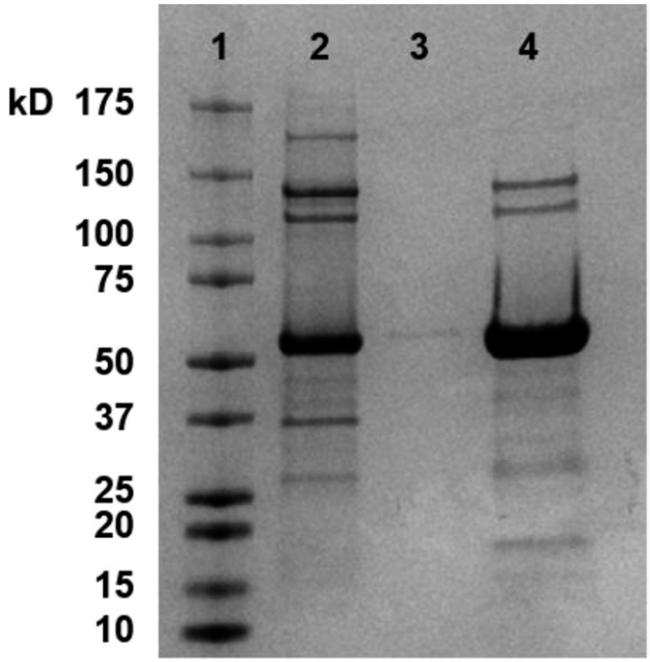

Fig. 3. Polyhistidine-Tag affinity purification of recombinant APOA5. Recombinant APOA5 was loaded onto a Ni Sepharose affinity column, washed with 60 mM imidazole, and eluted with 1 M imidazole. Eluate samples were analyzed by 4–15% SDS-PAGE and visualized with Coomassie blue. Samples were loaded by equal volume: lane 1, low molecular mass protein standards; lane 2, cleared lysate; lane 3, column wash fraction; lane 4, column elution fraction.

stepwise dialysis procedure into our screening buffer (10 mM HEPES, 0.15 M NaCl, 5 mM DTT, pH 7.8), the urea concentration of the protein sample in a denaturing HEPES buffer (10 mM HEPES, 0.15 M NaCl, 4 M urea, 5 mM DTT, pH 7.8) was brought to 3, 2, 1, and 0 M urea in 4 h increments, using 20× the sample volume. Our initial attempts to concentrate tAPOA5 in our screening buffer, using centrifugal spin filters, showed an unacceptably low solubility threshold of ~0.2 mg/ml, indicating that the fusion tags did not greatly improve APOA5 solubility at neutral pH. Therefore, we initiated a solubility screen to test multiple classes of buffers and additives to increase solubility. APOA5 in the screening buffer was dialyzed into each test buffer at 0.2 mg/ml. tAPOA5, which remained soluble in each test buffer after dialysis, was then concentrated by ultrafiltration and its protein concentration was measured until we noted signs of precipitation. **Table 1** shows a selection of buffers and additives that were screened. Only minor increases in protein solubility were observed with the addition of increased salt, organic compounds, amino acids, and detergents. However, tAPOA5 was found to be highly soluble in bicarbonate buffers at pH 7.8, as both ammonium bicarbonate and sodium bicarbonate buffers maintained tAPOA5 solubility up to concentrations of 10 mg/ml. In fact, the bicarbonate buffering systems were the only conditions that we screened that allowed the tAPOA5 protein concentration to exceed 0.31 mg/ml.

Fusion protein removal using TEV protease and affinity purification

After establishing a refolding protocol and a stable neutral buffer system for tAPOA5, we next focused on removing the fusion tags from the target protein. TEV protease effectively digested the fusion protein to leave an ~39 kDa mature APOA5 and the fusion tags at ~18 kDa (**Fig. 5**). The digested sample was then applied to a nickel affinity column to remove the liberated fusion tag. Unfortunately, we noted that APOA5 strongly and nonspecifically interacted with the affinity resin resulting in near complete sample loss. Optimization experiments in which the resin type and bed volume were modulated did not improve yield. Also, we varied buffer conditions (e.g., salt, pH, reducing agent, detergent, mild denaturation) without significant improvement. In the end, we found that the sample must be strongly denatured during purification with 6 M urea to prevent nonspecific association with the resin. This allowed the elution of largely pure mature APOA5 (Fig. 5). We worried that attempts to refold the mature APOA5 by dialyzing it back into a physiological buffer would result in precipitation due to its hydrophobic properties. Surprisingly, the untagged mature APOA5 exhibited excellent solubility in bicarbonate buffers. In fact, its solubility was comparable to the tagged version in this system.

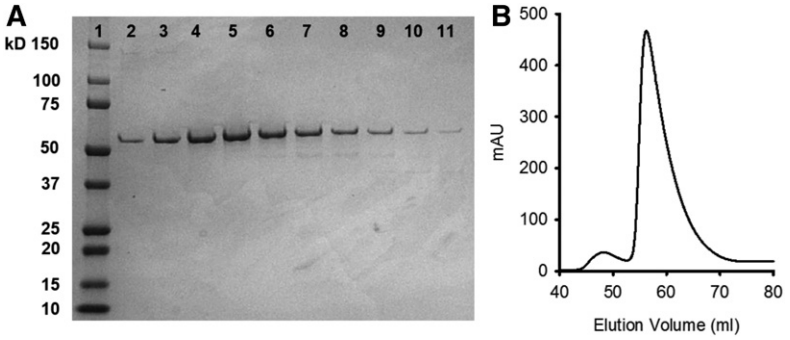

Fig. 4. SEC purification of recombinant APOA5. Analysis of SEC purification of tAPOA5 is shown here. A: Eluate fractions from SEC purification of tAPOA5 were analyzed by 4–15% SDS-PAGE and visualized with Coomassie blue. Samples were loaded by equal volume: lane 1, low molecular mass protein standards; lanes 2–11, elution fractions containing monomeric recombinant protein (elution volumes 54–69 ml). B: Chromatogram of SEC purification of tAPOA5 (elution volumes 40–80 ml).

Physical characterization of the recombinant protein

To determine the oligomeric state of mature APOA5 in ammonium bicarbonate buffer, we analyzed the sample by native PAGE. **Figure 6A** compares lipid-free APOA5 to lipid-free APOA1. APOA1 appeared as a smear of multimers of indeterminate molecular masses and diameters, as has been well-established in our laboratory and others. Similarly, APOA5 did not run as a homogenous population, suggesting that it also exists as multiple oligomeric species that are in a dynamic equilibrium. These data are consistent with analytical ultracentrifugation analyses, which did not support the existence of discrete oligomeric populations of lipid-free APOA5 in solution (data not shown). These findings are also consistent with SDS-PAGE analyses of chemically cross-linked lipid-free APOA5, which indicated the presence of multiple oligomeric species (Fig. 6B). We next performed a far UV CD analysis of mature APOA5 under both neutral and low pH conditions similar to those used by Beckstead et al. (12) (**Fig. 7**). APOA5 in acidic buffering conditions exhibited a spectrum typical of a helical protein with a calculated α-helicity of 37%, similar to previous reports (12). However, APOA5 in neutral buffering conditions exhibited an increase in α-helicity to 56%. Such differences in secondary structure suggest that APOA5 adopts a different structure in physiological buffering conditions that may more closely resemble the helical content of other lipid-free apolipoproteins (18).

Functional characterization of recombinant APOA5

To evaluate the functionality of the recombinant APOA5 produced in our system, we first measured its ability to solubilize multilamellar liposomes in a DMPC clearance assay. **Figure 8** shows that in the absence of protein, DMPC liposomes scattered significant light for the duration of the experiment. However, when APOA1 was added, the protein efficiently rearranged the multilamellar lipid structures into small discoidal particles that scattered less light. APOA5 also reorganized DMPC liposomes, though not as effectively as APOA1, at least on an equal protein mass basis, forming a heterogeneous array of particles as determined by native PAGE (data not shown). This indicates that APOA5 is surface active and likely properly folded for lipid interaction.

To determine whether our recombinant protein retained the ability to modulate plasma TG metabolism in vivo, we measured the ability of tAPOA5 to regulate postprandial plasma TG accumulation in WT C57BL/6J mice. After intragastric administration of a lipid bolus in fasted WT mice, we noted a postprandial elevation in plasma TG concentration from baseline (54 ± 6 mg/dl) by 30 min (98 ± 16 mg/dl) that was maintained up to 1 h (101 ± 20 mg/dl). Plasma TG concentration began decreasing by 2 h and returned to baseline by 3 h. Mice receiving intravenous injection of tAPOA5 1 h prior to intragastric lipid administration exhibited a significantly reduced postprandial plasma TG accumulation. In fact, plasma TG concentrations across all time points were not statistically different from the 0 h time point (0 h, 53 ± 4 mg/dl; 0.5 h, 65 ± 14 mg/dl; 1 h, 66 ± 12 mg/dl; 2 h, 57 ± 13 mg/dl; 3 h, 47 ± 9 mg/dl). Statistically significant ($P < 0.01$) changes in plasma TGs were observed at 0.5 and 1 h comparing control mice to those injected with tAPOA5 (**Fig. 9A**). Analysis of total plasma TG accumulation across all time points (i.e., area under the curve) showed a 2-fold increase ($P < 0.05$) in control mice (115 ± 26 mg/dl/min) compared with mice injected with tAPOA5 (56 ± 31 mg/dl/min) (Fig. 9B). In a separate experiment, mice treated with an intraperitoneal injection of tAPOA5 showed a similar reduction in postprandial plasma TG accumulation using the same experimental design (data not shown). Thus, administration of recombinant tAPOA5, in its lipid-free form, attenuated the postprandial TG accumulation in mouse plasma. These data are

TABLE 1. Solubility enhancement screening of tAPOA5 in various buffer conditions

Buffer	Additive	Solubility Threshold
HEPES[a]	—	0.2 mg/ml
HEPES	1 M NaCl	0.29 mg/ml
HEPES	10% Ethylene glycol v/v	0.21 mg/ml
HEPES	100 mM Glycine	0.22 mg/ml
HEPES	1 M Urea	0.24 mg/ml
HEPES	1% CHAPS v/v	0.31 mg/ml
HEPES	3% PEG 3350 w/v	<0.2 mg/ml
PBS[b]	—	0.28 mg/ml
Tris HCl[c]	—	0.22 mg/ml
Ammonium bicarbonate[d]	—	>10 mg/ml
Sodium bicarbonate[e]	—	>10 mg/ml

Recombinant tAPOA5 samples were dialyzed from HEPES buffer into experimental buffer conditions at 0.2 mg/ml, concentrated, and their protein concentrations were evaluated utilizing a Bradford protein assay.

[a]HEPES buffer: 10 mM HEPES, 150 mM NaCl, 5 mM DTT, pH 7.8.

[b]PBS buffer: 140 mM NaCl, 2.7 mM KCl, 10.1 mM Na_2HPO_4, 1.8 mM KH_2PO_4, 5 mM DTT, pH 7.4.

[c]Tris HCl buffer: 20 mM Tris HCl, 500 mM NaCl, 5 mM DTT, pH 7.8.

[d]Ammonium bicarbonate buffer: 10 mM NH_4HCO_3, 5 mM DTT, pH 7.8.

[e]Sodium bicarbonate buffer: 10 mM $NaHCO_3$, 5 mM DTT, pH 7.8.

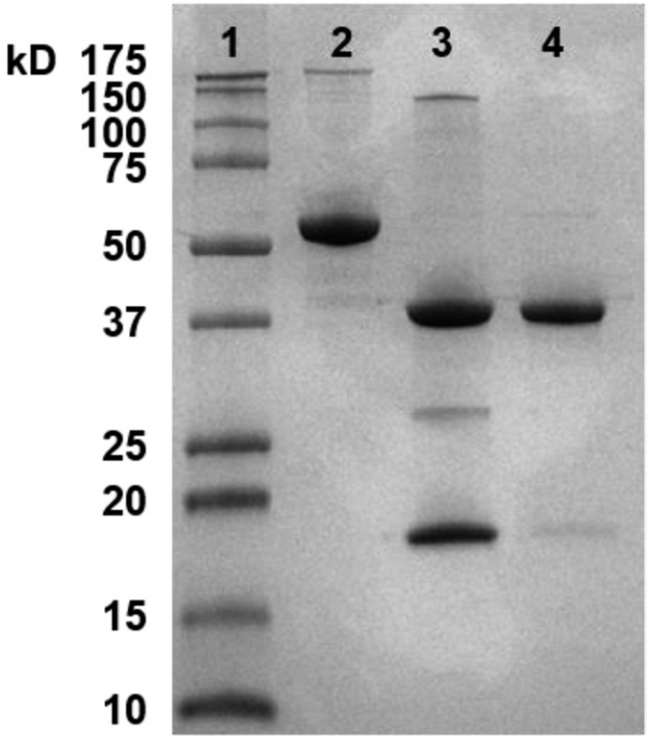

Fig. 5. Proteolytic cleavage and removal of N-terminal fusion tags from recombinant APOA5. Proteolytic removal of N-terminal fusion tags was performed at 4°C for 6 h utilizing TEV protease, and recombinant APOA5 was purified via nickel affinity chromatography under denaturing conditions (see text). APOA5 (6 μg) from each purification step was analyzed by 4–15% SDS-PAGE and visualized with Coomassie blue: lane 1, low molecular mass protein standards; lane 2, tAPOA5; lane 3, tAPOA5 digested with TEV protease; lane 4, purified APOA5.

consistent with previous functional evaluations of recombinant APOA5 utilizing similar methods, though in those cases, it was precomplexed with lipid due to the solubility issues of the protein at neutral pH (19).

DISCUSSION

This work shows that we successfully increased the bacterial production yield and solubility of human APOA5 at a physiological pH through: *i*) codon optimization, *ii*) addition of recombinant N-terminal fusion tags, *iii*) optimizing an efficient refolding protocol, and *iv*) screening of physiological buffer conditions. The resulting protein was biologically active in mice, capable of dramatically limiting the postprandial plasma TG response to a fatty meal. The finalized laboratory protocol for this expression and isolation is provided in supplementary materials.

Bacterial expression systems provide a cost-effective and high-throughput means of heterologous protein production; however, recombinant protein yield can be dramatically limited by numerous factors during expression (e.g., expression vector performance, proteolytic degradation). Although the mechanism(s) are poorly understood, the TRX-Tag has been reported to enhance the expression yield of its fusion partners (20). Due to its high solubility,

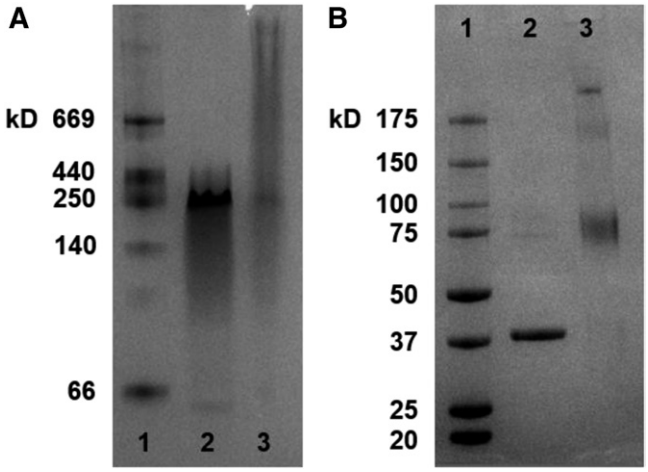

Fig. 6. Analysis of oligomeric distribution of APOA5. The oligomeric distribution of lipid-free APOA5 was evaluated utilizing native PAGE analysis and SDS-PAGE analysis of BS^3 cross-linked protein. A: Recombinant APOA1 and APOA5 were analyzed by 4–15% native PAGE and visualized with Coomassie blue. Samples were loaded by equal protein mass (5 μg): lane 1, high molecular mass native protein standards; lane 2, APOA1; lane 3, APOA5. B: Recombinant APOA5, cross-linked with BS^3, was analyzed by 4–15% SDS-PAGE and visualized with Coomassie blue. Samples were loaded by equal protein mass (5 μg): lane 1, low molecular mass protein standards; lane 2, APOA5; lane 3, cross-linked APOA5.

the TRX-Tag may decrease aggregation during protein elongation, thus increasing APOA5 expression by possibly limiting the negative effects of its extreme hydrophobicity during production. Given reports of the susceptibility of APOA5 to degradation by Beckstead et al. (12), the TRX-Tag may also increase yield by preventing proteolysis during expression in *E. coli* (21).

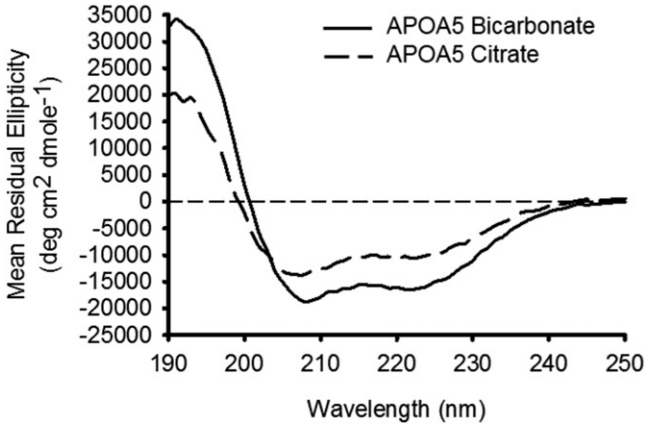

Fig. 7. Far UV CD spectra of recombinant APOA5 at acidic and neutral pH. Far UV CD was performed to analyze the secondary structure of APOA5 in bicarbonate buffer (pH 7.8) (56% α-helix, 8% β-sheet, 13% β-turn, 23% random coil) compared with citrate buffer (pH 3.0) (37% α-helix, 17% β-sheet, 20% β-turn, 28% random coil) as described in the Materials and Methods. Data show the mean residual ellipticity of APOA5 from 190 to 250 nm. The spectra shown are averages of two independent preparations of protein, each run in triplicate (n = 6 individual runs).

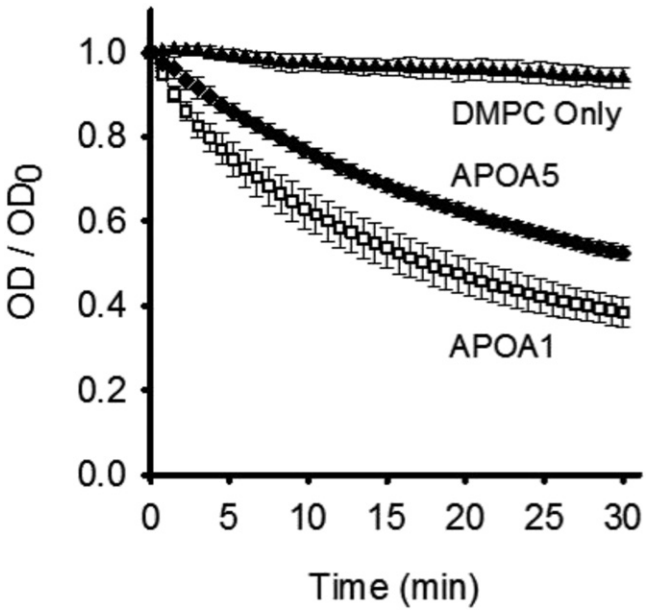

Fig. 8. DMPC clearance assay of APOA5 versus APOA1. A DMPC liposome solubilization assay was performed to characterize lipid association and reorganization properties of recombinant APOA5 compared with APOA1. Sample solutions were prepared on equal mass ratio of 2.5:1 DMPC to protein (106 μg DMPC:42.4 μg protein). Samples were run at 24.5°C, the transition temperature of DMPC, for 30 min with readings every 15 s (every third data point shown). Fractional absorbance was calculated as OD divided by the initial OD (OD_0). Values are expressed as mean ± SD (n = 5).

When contemplating solubility-enhancing strategies for APOA5 under physiological pH conditions, it is important to identify those characteristics that may favor protein aggregation (i.e., modes of self-association that result in protein precipitation) versus the normal soluble oligomerization interactions commonly observed among exchangeable apolipoproteins. The overall hydrophobicity of APOA5 is likely a factor promoting insolubility in neutral pH systems, as it is predicted to be more hydrophobic than both APOA1 and APOA4, despite sharing high levels of α-helical structure (12). Also, it is well-documented that regions of high surface charge density can act as nucleation centers for unfolding and subsequent aggregation (22). Analysis of the charge distribution of the primary sequence of APOA5 suggests two regions of concentrated positive charge (i.e., amino acids 170-186 and 197-245), which may weaken secondary structure due to electrostatic repulsion between sidechains (EMBOSS Charge, data not shown). Previous studies of APOA5 have also suggested that regions between amino acids 186 and 238 are critical in heparan sulfate proteoglycan binding, cell membrane receptor binding, and lipid binding (11, 23, 24). We propose that, due to the high concentration of positively charged residues and lipid-emulsifying properties of this region, APOA5 is susceptible to misfolding during bacterial translation, which contributes to protein aggregation/insolubility when APOA5 is purified and subjected to neutral pH. We suggest that our approach of strong denaturation followed by a stepwise removal of the denaturant likely minimized the formation of aberrant conformations and promoted those which, when presented the proper buffer system, favor solubility at a neutral pH. The hydrophobic properties of APOA5 seem to require the use of strong denaturants in order to prevent protein loss during the chromatography steps of its purification. Thus, our protocol was designed to denature the protein immediately after expression, maintain it in a denatured state during purification, and then allow it to refold gradually as it is dialyzed into a solubility-enhancing bicarbonate buffer.

Buffering conditions can have a dramatic effect on protein stability in an aqueous environment (25). Many anionic compounds, with a high density of negative charge, have been shown to increase protein stability (26). The results of our buffer optimization screen suggested that bicarbonate buffers greatly enhance APOA5 stability in neutral pH systems. One way that the negatively charged polyatomic bicarbonate ion may have prevented APOA5 aggregation is by stabilizing its secondary structure through interactions on the protein-buffer interface, possibly in the heparan sulfate proteoglycan binding region or other regions containing a high localization of positive charge.

Due to the limited solubility of APOA5 reported in previous studies, analyses of its physical properties (e.g., secondary structure, lipid binding, thermal stability) were performed under acidic buffering conditions (12). Our work here shows a substantial difference in secondary structure between

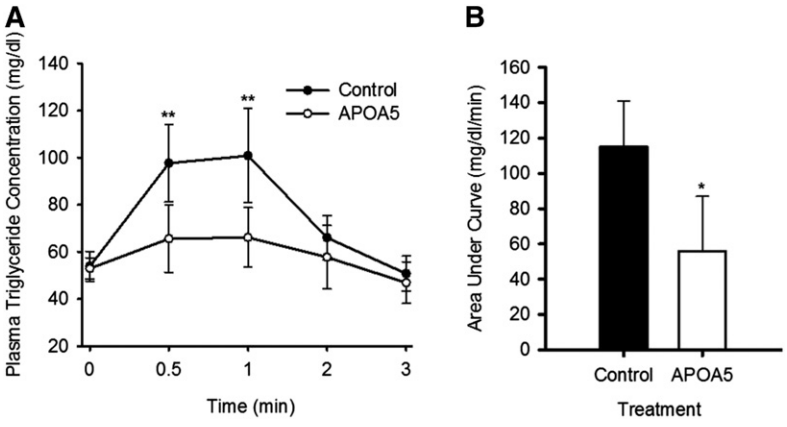

Fig. 9. Postprandial plasma TG regulation of lipid-free recombinant APOA5 intravenously injected in WT C57BL/6J mice. Effect of intravenous injection of lipid-free tAPOA5 on postprandial plasma TG concentration in WT C57BL/6J mice orally gavaged with 10% Intralipid is shown. Mice were injected with vehicle buffer (filled circles) or tAPOA5 (open circles) 1 h prior to oral gavage of Intralipid. Plasma samples were isolated from the tail vein at 0, 0.5, 1, 2, and 3 h post gavage and analyzed for TGs. A: Plasma TG concentration (milligrams per deciliter) of vehicle and tAPOA5-treated mice at each time point after oral gavage. B: Total plasma TGs, area under the curve (milligrams per deciliter per minute), for both control and tAPOA5-treated mice across all time points. Values are expressed as mean ± SD (n = 5 mice per group). Student's *t*-test results versus the respective controls were as follows: $^*P < 0.05$, $^{**}P < 0.01$.

neutral and acidic buffering conditions. This is not surprising, as pH-induced alterations in secondary structure have been described for other proteins (27). However, the fact that we can now produce high concentrations of APOA5 under conditions of physiological pH opens new possibilities for structural and functional studies of this protein. For example, this conformational state may be more amenable to protein crystallization for high-resolution X-ray crystallography studies, which are ongoing in our laboratory. Importantly, this work also opens the door to the use of lipid-free APOA5 in mice without the requirement of precomplexation to lipid in order to maintain its solubility in neutral plasma. Furthermore, site-directed mutagenesis studies designed to identify functional regions within APOA5 will be facilitated by the high yield and long-term stability of mutants generated under this protocol. Finally, we can now study the structural transitions that APOA5 undergoes during lipoprotein particle assembly or exchange between lipoproteins, such as transfers between HDL and VLDL and vice versa, which likely occur at neutral pH.

To summarize, we describe a novel APOA5 production system with a robust protein yield that maintains solubility under physiological buffering conditions at high concentrations in a lipid-free state. Functional characterization showed that our recombinant APOA5 is surface active and can significantly reduce postprandial plasma TG accumulation in vivo. With the ability to generate ample material in physiological buffering conditions, this expression system should facilitate ongoing studies of how APOA5 structure relates to its function in TG metabolism.

The authors thank Dr. Robert O. Ryan for the donation of the pET20b(+) APOA5 expression vector.

REFERENCES

1. Pennacchio, L. A., M. Olivier, J. A. Hubacek, J. C. Cohen, D. R. Cox, J. Fruchart, R. M. Krauss, and E. M. Rubin. 2001. An apolipoprotein influencing triglycerides in humans and mice revealed by comparative sequencing. *Science.* **294:** 169–173.
2. O'Brien, P. J., W. E. Alborn, J. H. Sloan, M. Ulmer, A. Boodhoo, M. D. Knierman, A. E. Schultze, and R. J. Konrad. 2005. The novel apolipoprotein A5 is present in human serum, is associated with VLDL, HDL, and chylomicrons, and circulates at very low concentrations compared with other apolipoproteins. *Clin. Chem.* **51:** 351–359.
3. Merkel, M., B. Loeffler, M. Kluger, N. Fabig, G. Geppert, L. A. Pennachio, A. Laatsch, and J. Heeren. 2005. Apolipoprotein AV accelerates plasma hydrolysis of triglyceride-rich lipoproteins by interactions with proteoglycan-bound lipoprotein lipase. *J. Biol. Chem.* **280:** 21553–21560.
4. Grosskopf, I., N. Baroukh, S. Lee, Y. Kamari, D. Harats, E. M. Rubin, L. A. Pennacchio, and A. D. Cooper. 2005. Apolipoprotein A-V deficiency results in marked hypertriglyceridemia attributable to decreased lipolysis of triglyceride-rich lipoproteins and removal of their remnants. *Arterioscler. Thromb. Vasc. Biol.* **25:** 2573–2579.
5. Shu, X., L. Nelbacha, R. O. Ryan, and T. M. Forte. 2010. Apolipoprotein A-V associates with intrahepatic lipids droplets and influences triglyceride accumulation. *Biochim. Biophys. Acta.* **1801:** 605–608.
6. Ishihara, M., T. Kujiraoka, T. Iwasaki, M. Nagano, M. Takano, J. Ishii, M. Tsuji, H. Ide, I. P. Miller, N. E. Miller, et al. 2005. A sandwich enzyme-linked immunosorbent assay for human plasma apolipoprotein A-V concentration. *J. Lipid Res.* **46:** 2015–2022.
7. Wong, K., and R. O. Ryan. 2007. Characterization of apolipoprotein A-V structure and mode of plasma triacylglycerol regulation. *Curr. Opin. Lipidol.* **18:** 319–324.
8. Alborn, W. E., M. G. Johnson, M. J. Prince, and R. J. Konrad. 2006. Definitive n-terminal protein sequence and further characterization of the novel apolipoprotein A5 in human serum. *Clin. Chem.* **52:** 514–517.
9. Mendoza-Barberá, E., J. Julve, S. K. Nilsson, A. Lookene, J. M. Martin-Campos, R. Roig, A. M. Lechuga-Sancho, J. H. Sloan, P. Fuentes-Prior, and F. Blanco-Vaca. 2013. Structural and functional analysis of APOA5 mutations identified in patients with severe hypertriglyceridemia. *J. Lipid Res.* **54:** 649–661.
10. Weinberg, R. B., V. R. Cook, J. A. Beckstead, D. D. O. Martin, J. W. Gallagher, G. S. Shelness, and R. O. Ryan. 2003. Structure and interfacial properties of human apolipoprotein A-V. *J. Biol. Chem.* **278:** 34438–34444.
11. Sun, G., N. Bi, G. Li, X. Zhu, W. Zeng, G. Wu, H. Xue, and B. Chen. 2006. Identification of lipid-binding and lipoprotein lipase activation domains of human apoAV. *Chem. Phys. Lipids.* **143:** 22–28.
12. Beckstead, J. A., M. N. Oda, D. D. O. Martin, T. M. Forte, J. K. Bielicki, T. Berger, R. Luty, C. M. Kay, and R. O. Ryan. 2003. Structure-function studies of human apolipoprotein A-V: a regulator of plasma lipid homeostasis. *Biochemistry.* **42:** 9416–9423.
13. Forte, T. M., and R. O. Ryan. 2015. Apolipoprotein A5: extracellular and intracellular roles in triglyceride metabolism. *Curr. Drug Targets.* **16:** 1274–1280.
14. Sreerama, N., and R. W. Woody. 2000. Estimation of protein secondary structure from CD spectra: comparison of CONTIN, SELCON, and CDSSTR methods with an expanded reference set. *Anal. Biochem.* **287:** 252–260.
15. Lobley, A., L. Whitmore, and B. A. Wallace. 2002. DICHROWEB: an interactive website for the analysis of protein secondary structure from circular dichroism spectra. *Bioinformatics.* **18:** 211–212.
16. Raab, D., M. Graf, F. Notka, T. Schödl, and R. Wagner. 2010. The GeneOptimizer algorithm: using a sliding window approach to cope with the vast sequence space in multiparameter DNA sequence optimization. *Syst. Synth. Biol.* **4:** 215–225.
17. Young, C. L., Z. T. Britton, and A. S. Robinson. 2012. Recombinant protein expression and purification: a comprehensive review of affinity tags and microbial applications. *Biotechnol. J.* **7:** 620–634.
18. Tubb, M. R., L. E. Smith, and W. S. Davidson. 2009. Purification of recombinant apolipoproteins A-I and A-IV and efficient affinity tag cleavage by tobacco etch virus protease. *J. Lipid Res.* **50:** 1497–1504.
19. Shu, X., L. Nelbach, M. W. Weinstein, B. L. Burgess, J. A. Beckstead, S. G. Young, R. O. Ryan, and T. M. Forte. 2010. Intravenous injection of apolipoprotein A-V reconstituted high-density lipoprotein decreases hypertriglyceridemia in apoav−/− mice and requires glycosylphosphatidylinositol-anchored high-density lipoprotein-binding protein 1. *Arterioscler. Thromb. Vasc. Biol.* **30:** 2504–2509.
20. Mierendorf, R. C., B. B. Morris, B. Hammer, and R. E. Novy. 1998. Expression and purification of recombinant proteins using the pET system. *In* Molecular Diagnosis of Infectious Diseases: Methods in Molecular Medicine. U. Reischl, editor. Humana Press, Totowa, NJ. 257–292.
21. Li, H., X. Hui, K. Li, X. Tang, X. Hu, A. Xu, and D. Wu. 2014. High-level expression, purification, and characterization of active human C1q and tumor necrosis factor-related protein-1 in Escherichia coli. *Lett. Appl. Microbiol.* **59:** 334–341.
22. McPhail, D., and C. Holt. 2001. Effects of anions on the denaturation and aggregation of b-lactoglobulin as measured by differential scanning microcalorimetry. *Int. J. Food Sci. Technol.* **34:** 477–481.
23. Su, X., Y. Kong, and D. Peng. 2018. New insights into apolipoprotein A5 in controlling lipoprotein metabolism in obesity and the metabolic syndrome patients. *Lipids Health Dis.* **17:** 174.
24. Gin, P., A. P. Beigneux, B. Davies, M. F. Young, R. O. Ryan, A. Bensadoun, L. G. Fong, and S. G. Young. 2007. Normal binding of the lipoprotein lipase, chylomicrons, and apo-AV to GPIHBP1 containing G56R amino acid substitution. *Biochim. Biophys. Acta.* **1771:** 1464–1468.
25. Ugwu, S. O., and S. P. Apte. 2004. The effect of buffers on protein conformational stability. *Pharm. Technol.* **28:** 86–113.
26. Broering, J. M., and A. S. Bommarius. 2005. Evaluation of Hofmeister effects on the kinetic stability of proteins. *J. Phys. Chem. B.* **109:** 20612–20619.
27. Kumar, D. P., A. Tiwari, and R. Bhat. 2004. Effect of pH on the stability and structure of yeast hexokinase a. *J. Biol. Chem.* **279:** 32093–32099.